Bioorganic & Medicinal Chemistry Letters 20 (2010) 2687–2704

Contents lists available at ScienceDirect

Bioorganic & Medicinal Chemistry Letters

journal homepage: www.elsevier.com/locate/bmcl

Bioorganic & Medicinal Chemistry Letters Volume 20, Issue 9, 2010

Contents

ARTICLES

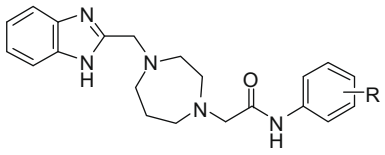

4a-s

We have synthesized and biologically evaluated 1,4-diazepane derivatives as T-type calcium channel blockers. In this study, we discovered compound **4s**, a potential T-type calcium channel blocker with good selectivity over hERG and N-type calcium channels. In addition, it exhibited favorable pharmacokinetic characteristics for further investigation of T-type calcium channel related diseases.

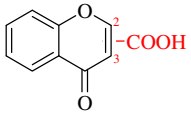

Docking experiments were carried out to explain the quite different inhibition activities of two carboxylic chromone isomers against A and B isoforms of monoamine oxidases.

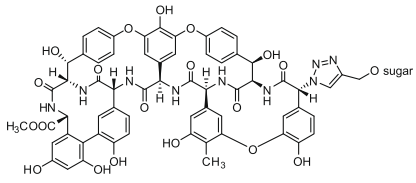

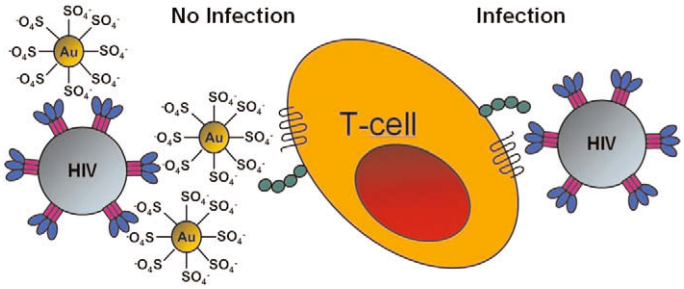

A golden opportunity against HIV. Gold nanoparticles coated with multiple copies of an amphiphilic sulphate-ended ligand inhibit in vitro the HIV infection of T-cells at nanomolar concentrations.

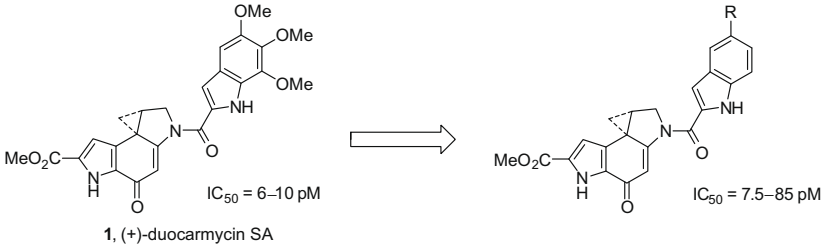

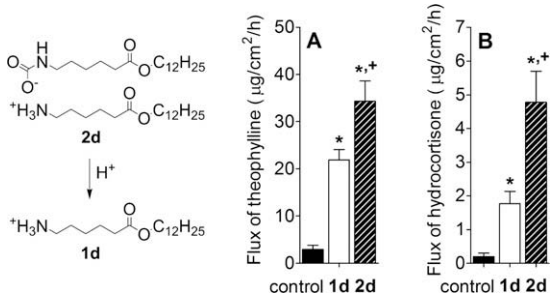

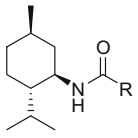

R = Aryl, Alkyl, $(CH_2)_nPh$, OAryl, NHAlkyl

The evaluation of a series of (−)-menthylamine derivatives led to the identification of some potent TRPM8 antagonists with IC_{50} values versus icilin and (−)-menthol between 20 nM and 0.7 μM and between 4- and ~150-fold selective versus TRPV1 and TRPA1 activation.

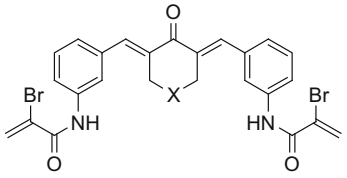

X=NR with R=Bn, CO_2Me, CO_2Et
or
X=(CH_2)n with n=1, 2 or 3

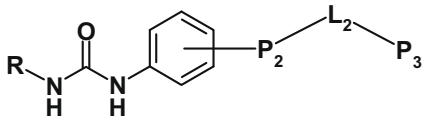

1

The impact of various secondary and tertiary pharmacophores on in vitro potency of soluble epoxide hydrolase (sEH) inhibitors based on the unsymmetrical urea scaffold **1** is discussed.

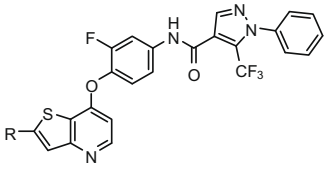

A novel series of *N*-(3-fluoro-4-(2-substituted-thieno[3,2-*b*]pyridin-7-yloxy)phenyl)-1-phenyl-5-(trifluoromethyl)-1*H*-pyrazole-4-carboxamides targeting RON receptor tyrosine kinase was designed and synthesized. SAR study of the series allowed us to identify compounds possessing either inhibitory activity of RON kinase enzyme in the low nanomolar range with low residual activity against the closely related c-Met or potent dual inhibitory activity against RON and c-Met, – with no significant activity against VEGFR2 in both cases.

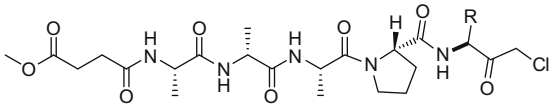

a, R = $CHMe_2$, **6a**: 82%
b, R = CH_2CHMe_2, **6b**: 84%

The synthesis and biological evaluation of modified pentapeptides **6a** and **6b** are described as potent proteinase K inhibitors.

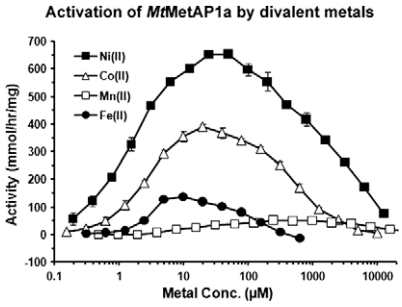

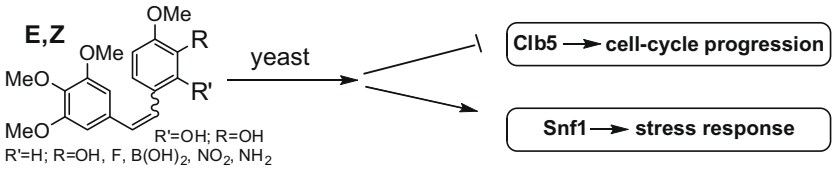

To enlighten new anti-tumor activities, a series of combretastatin A-4 derivatives and combretastatin A-1 were prepared and evaluated in arresting yeast growth. The G1 arrest induced by some of these compounds was characterized by the down-regulation of G1 cyclin Clb5 and activation of the stress activated kinase Snf1.

The original structure assignment of **2**, a high-throughput screening hit obtained from an external vendor, was revised based on multiple NMR studies. A novel synthetic route was developed for **2** and multi-gram quantities were prepared for pharmacokinetic and efficacy studies. Its activity on the BRS-3 receptor was confirmed, and additional SAR was explored.

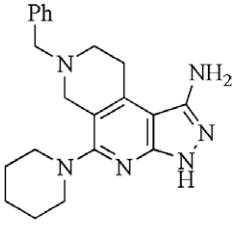

2

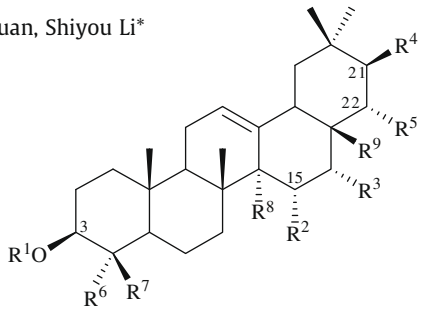

Some cytotoxic polyhydroxylated oleananes inhibited DNA topoisomerase I (TOP1) catalytic activity by interacting directly with the free enzyme and preventing the formation of the DNA–TOP1 complex.

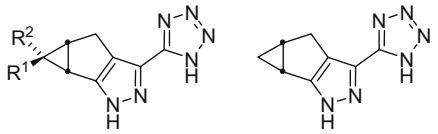

(+)**17a**

Tricyclic pyrazole tetrazoles which are potent partial agonists of the high affinity niacin receptor, GPR109a, have been discovered and optimized. One of these compounds has proven to be effective at lowering free fatty acids in vitro and in vivo.

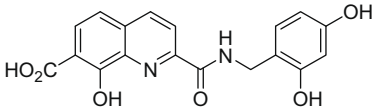

IC_{50} = 200 nM

2-Substituted 8-hydroxy-quinoline-7-carboxylic acid compounds have been identified as small molecule inhibitors of the Pim-1 kinase and molecular docking studies have shown their potential binding mode.

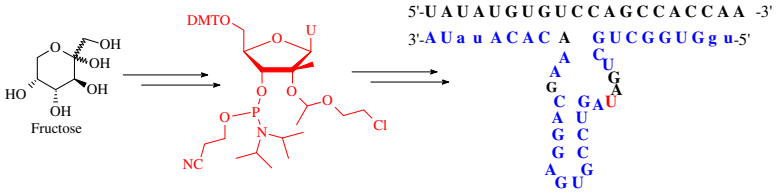

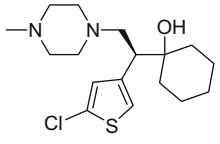

(+)-S-21

A series of heterocyclic cycloalkanol ethylamines have been prepared to expand our norepinephrine reuptake inhibitor (NRI) program. Synthesis of a variety of heterocycles identified (+)-*S*-**21**, a potent NRI efficacious in an animal model for thermoregulatory dysfunction.

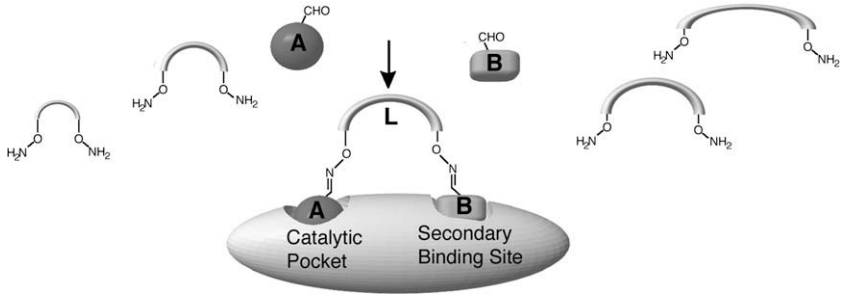

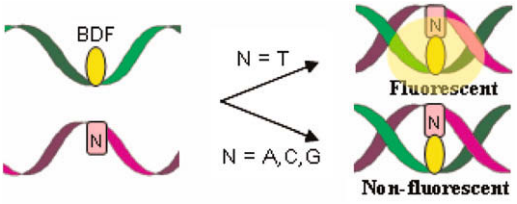

Distinction of thymine base by BDF probe

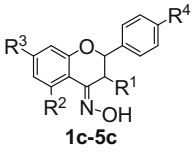

1c-5c

1 R^1=R^4=H, R^2=OH, R^3=OCH_3
2 R^1=R^3=OCH_3, R^2=OH, R^4=H
3 R^1=R^4=H, R^2=R^3=OCH_3
4 R^1=H, R^2=R^3=R^4=OCH_3
5 R^1=R^4=H, R^2=R^3=OH

Structural modification of flavones isolated from *Kaempferia parviflora* afforded 16 flavonoid derivatives. Oxime **1c** exhibited dramatically strong cytotoxicity against KB and NCI-H187 cell lines with IC_{50} values of 0.26 and 0.014 μM, respectively, while **2c** showed strong cytotoxicity against NCI-H187 cell line with an IC_{50} value of 0.23 μM.

A series of arylbutanoids and diarylheptanoids was isolated from the bark of *Betula platyphylla*. These compounds showed significant inhibitory activity against antigen-induced degranulation of RBL-2H3 cells.

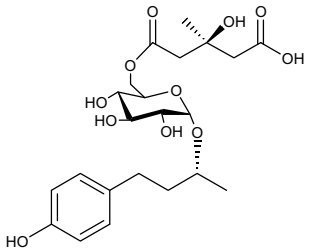

4

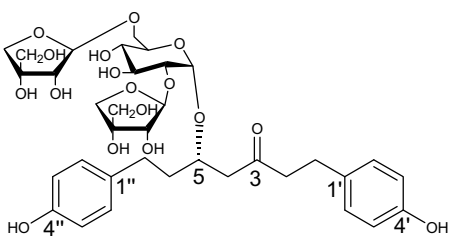

12

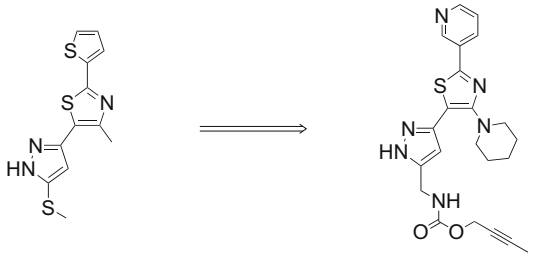

E. coli Ki = 2.2 μM *E. coli* Ki < 0.004 μM

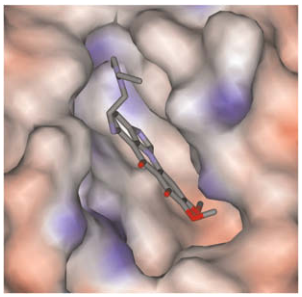

Electrostatic surface representation of NQO2 with **NSC660841** docked in the binding pocked. **NSC660841** is identified as the most potent inhibitor of NQO2 yet reported (IC_{50} = 6 nM).

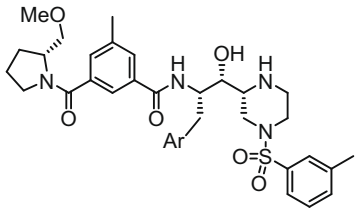

Design and optimization of a novel series of piperazine sulfonamide inhibitors of BACE1 are described, with an emphasis on SAR of the non-prime side and S2′ binding motifs. The lead inhibitor demonstrated a prolonged inhibition of peripheral $A\beta_{40}$ in transgenic mice with a single acute dose.

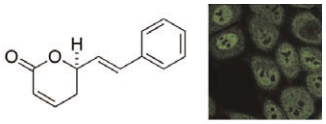

(*R*)-Goniothalamin
Inhibitor of Nuclear Export

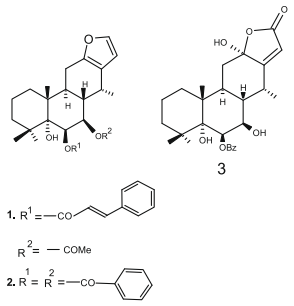

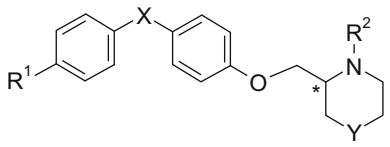

Novel piperidine and piperazine derivatives have been designed and tested as inhibitors of LTA_4 hydrolase (LTA_4H). Most potent compounds showed good potency in both enzymatic and functional human whole blood assay. Crystallography studies further confirmed observed structure–activity relationship and LTA_4H binding mode for analogs from the piperidine series.

Structure of CAB-SHZH27 and its dose-dependent cytotoxicity on MDA-MB-231 cells.

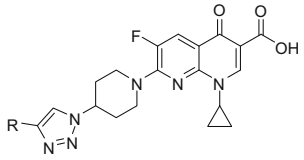

R = Ph, CH_2OH, CH_2NH_2, $COOCH_3$, $CONH_2$, CHO, $CH(CH_3)OH$, $CH(C_2H_5)OH$, CHNOH, $CHNOCH_3$, $CHNOC_2H_5$, $CHNOCH_2CHCH_2$, $CHNOCH_2CCH$, CHNOBn, etc.

A series of novel quinolones based on 4-substituted 4-(1*H*-1,2,3-triazol-1-yl)piperidine as the C7 building blocks of quinolone core 7-chloro-1-cyclopropyl-6-fluoro-4-oxo-1,4-dihydro-1,8-naphthyridine-3-carboxylic acid was synthesized. The antibacterial activity of these new fluoroquinolones was evaluated by standard broth microdilution technique. Among them, the quinolone 1-cyclopropyl-6-fluoro-7-(4-(4-formyl-1*H*-1,2,3-triazol-1-yl)piperidin-1-yl)-4-oxo-1,4-dihydro-1,8-naphthyridine-3-carboxylic acid exhibited comparable antibacterial activity against quinolone-susceptible and multidrug-resistant strains in comparison with ciprofloxacin and vancomycin, especially to *Staphylococcus aureus* and *Staphylococcus epidermidis*.

A novel series of arylindenopyrimidines were identified as A_{2A} and A_1 receptor antagonists. The series was optimized for in vitro activity by substituting the 8- and 9-positions with methylene amine substituents. The compounds show excellent activity in mouse models of Parkinson's disease when dosed orally.

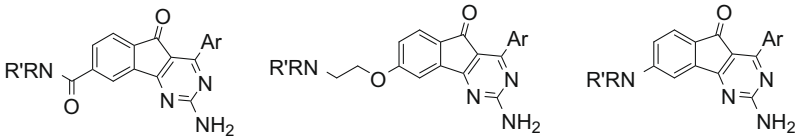

Two reactive metabolites were identified in vivo for the dual A_{2A}/A_1 receptor antagonist **1**. Two strategies were implemented to successfully mitigate the metabolic liabilities associated with **1**. Optimization of the arylindenopyrimidines led to a number of amide, ether, and amino analogs having comparable in vitro and in vivo activity.

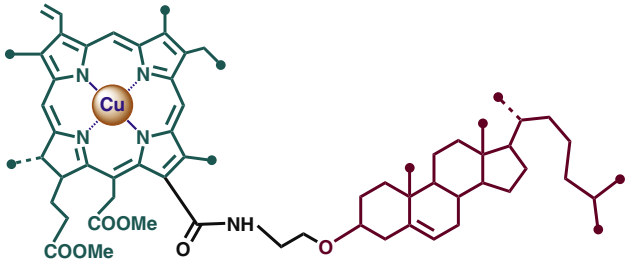

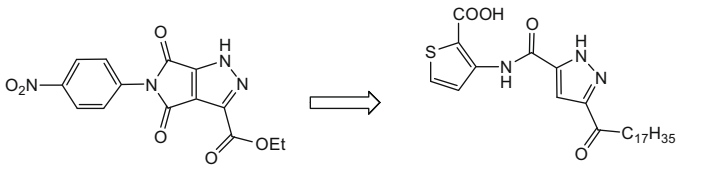

1, HTS hit, IC_{50} 32 μM for Cdc25B

118 IC_{50}=0.12 μM for Cdc25B

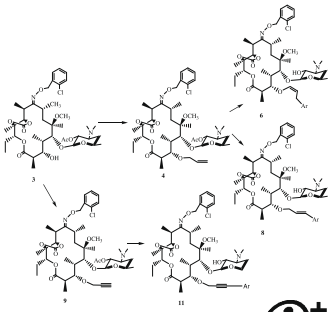

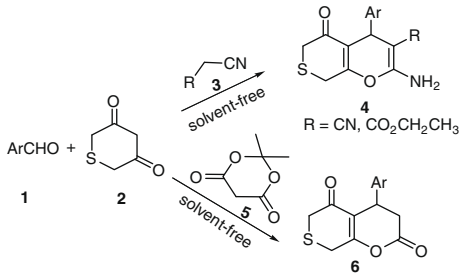

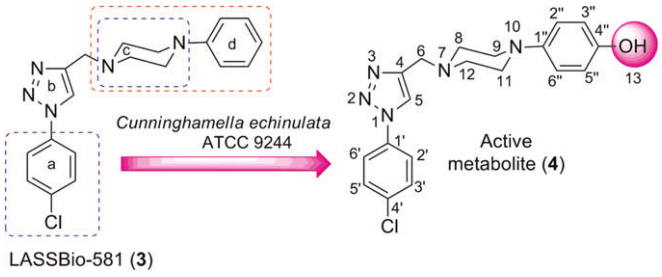

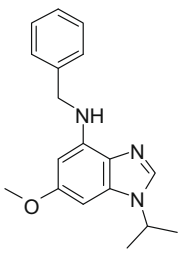

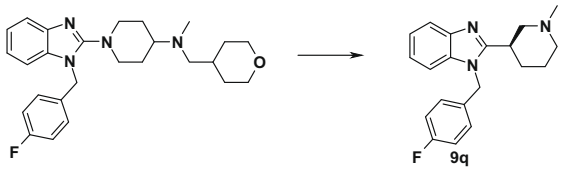

A series of 2-(piperidin-3-yl)-1*H*-benzimidazoles were identified as selective H_1-antihistamines for evaluation as potential sedative hypnotics. Representative compounds showed generally improved hERG selectivity over a previously identified 2-aminobenzimidazole series. While hERG activity could be modulated via manipulation of the benzimidazole N1 substituent, this approach led to a reduction in CNS exposure for the more selective compounds. One example, **9q**, retained a suitable selectivity profile with CNS exposure equivalent to known centrally active H_1-antihistamines.

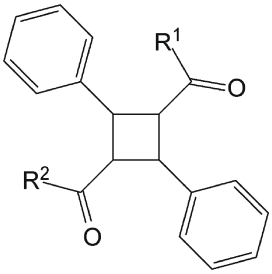

Structure-activity relationships of truxillic acid derivatives as subtype-selective PPARγ activators are presented.

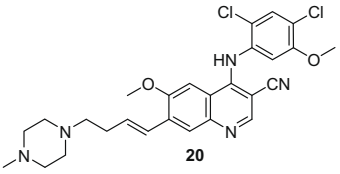

The 7-alkene-3-quinolinecarbonitrile **20**, a potent inhibitor of Src enzymatic and cellular activity with IC_{50} values of 2.1 and 58 nM, respectively, had comparable efficacy to bosutinib in a colon tumor xenograft study.

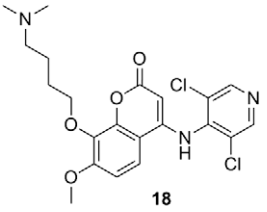

The development of a novel series of water-soluble PDE4 inhibitors led to the discovery of coumarin **18**, which is effective in a rabbit model of dry eye and a tear secretion test in rats.

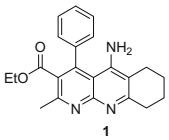

1

eeAChE (IC_{50})= 822 nM

eqBuChE (IC_{50})= 5.03 ± 0.57 μM

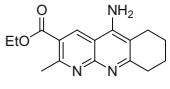

2

eeAChE (IC_{50})= 60 ± 0.006 nM

hAChE (IC_{50})= 780 ± 0.08 nM

eqBuChE (IC_{50})= 12 ± 1 μM

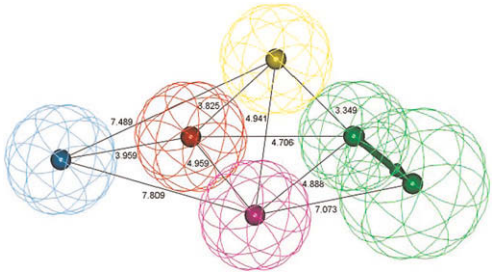

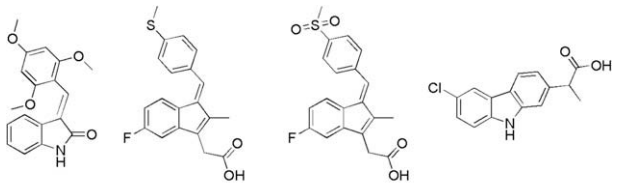

1, IC261 2, Sulindac-S 3, Sulindac-Sulfone 4, Carprofen

Structural similarity of IC261 and the GSM of the Sulindac-series (**2**, **4**).

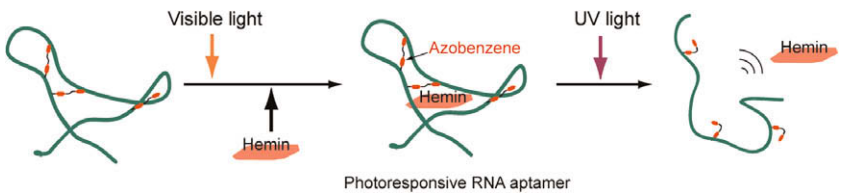

In vitro selection of photoresponsive RNA aptamer against hemin was reported.

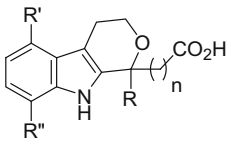

We describe the structure–activity relationship of the C1-group of pyrano[3,4-*b*]indole based inhibitors of HCV NS5B polymerase. Further exploration of the allosteric binding site led to the discovery of the significantly more potent compound **12**.

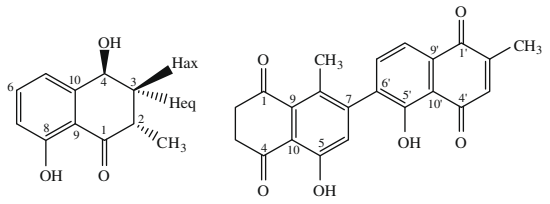

4 **8**

Bioassay guided isolation of mosquitocidal extract of *P. capensis* rhizomes yielded two new napthaquinones, isoplumbagolone (**4**) and chitranane (**8**) along with six known compounds (**1**–**3**, **5**–**7**) as a mosquitocidal constituents, possessing varying degree of mosquitocidal potentials.

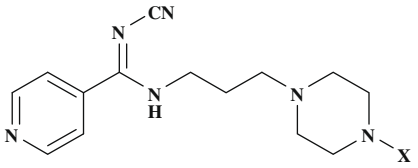

N′-Cyanoisonicotinamidine derivatives, linked to an arylpiperazine moiety, were prepared to identify highly selective and potent 5-HT$_{1A}$ ligands. *N*′-Cyano-*N*-(3-(4-(pyridin-2-yl)piperazin-1-yl)propyl)isonicotinamidine (**4o**) with K_i = 0.038 nM, was the most active and selective derivative for the 5-HT$_{1A}$ receptor.

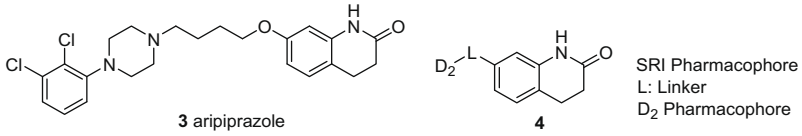

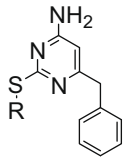

A number of novel 2-arylalkylthio-4-amino-6-benzyl pyrimidines were designed and synthesized as potent NNRTIs. The results showed that the changes of $N_3H–C_4=O$ into $N_3=C_4–NH_2$ could increase the activity.

*Corresponding author
ⓘ+ Supplementary data available via ScienceDirect

COVER

Overlay of high resolution co-crystal structures of *R*-**22**-ADP (cyan) and **1**-ADP (green) bound in an allosteric binding site of the mitotic kinesin KSP. [Roecker, A. J.; Coleman, P. J.; Mercer, S. P.; Schreier, J. D.; Buser, C. A.; Walsh, E. S.; Hamilton, K.; Lobell, R. B.; Tao, W.; Diehl, R. E.; South, V. J.; Davide, J. P.; Kohl, N. E.; Yan, Y.; Kuo, L. C.; Li, C.; Fernandez-Metzler, C.; Mahan, E. A.; Prueksaritanont, T.; Hartman, G. D. *Bioorg. Med. Chem. Lett.* **2007**, *17*, 5677.]

Indexed/Abstracted in: Beilstein, Biochemistry & Biophysics Citation Index, CANCERLIT, Chemical Abstracts, Chemistry Citation Index, Current Awareness in Biological Sciences/BIOBASE, Current Contents: Life Sciences, EMBASE/Excerpta Medica, MEDLINE, PASCAL, Research Alert, Science Citation Index, SciSearch, TOXFILE. Also covered in the abstract and citation database SCOPUS®. Full text available on ScienceDirect®

ELSEVIER

ISSN 0960-894X